# A Bayesian framework to identify random parameter fields based on the copula theorem and Gaussian fields: Application to polycrystalline materials

H. Rappel[a], L. Wu[b], L. Noels[b], L.A.A. Beex[a,*]

[a] *Institute of Computational Engineering, Faculty of Science, Technology and Communication, University of Luxembourg, Maison du Nombre, 6, Avenue de la Fonte, 4364, Esch-sur-Alzette, Luxembourg.*

[b] *Computational & Multiscale Mechanics of Materials (CM3), Department of Aerospace and Mechanical Engineering, University of Liège, Quartier Polytech 1, Allée de la Découverte 9, B-4000 Liège, Belgium.*

**Abstract**

For many models of solids, we frequently assume that the material parameters do not vary in space, nor that they vary from one product realization to another. If the length scale of the application approaches the length scale of the micro-structure however, spatially fluctuating parameter fields (which vary from one realization of the field to another) can be incorporated to make the model capture the stochasticity of the underlying micro-structure. Randomly fluctuating parameter fields are often described as Gaussian fields. Gaussian fields however assume that the probability density function of a material parameter at a given location is a univariate Gaussian distribution. This entails for instance that negative parameter values can be realized, whereas most material parameters have physical bounds (e.g. the Young's modulus cannot be negative). In this contribution, randomly fluctuating parameter fields are therefore described using the copula theorem and Gaussian fields, which allow different types of univariate marginal distributions to be incorporated, but with the same correlation structure as Gaussian fields. It is convenient to keep the Gaussian correlation structure, as it allows us to draw samples from Gaussian fields and transform them into the new random fields. The benefit of this approach is that any type of univariate marginal distribution can be incorporated. If the selected univariate marginal distribution has bounds, unphysical material parameter values will never be realized. We then use Bayesian inference to identify the distribution parameters (which govern the random field). Bayesian inference regards the parameters that are to be identified as random variables and requires a user-defined prior distribution of the parameters to which the observations are inferred. For the homogenized Young's modulus of a columnar polycrystalline material of interest in this study, the results show that with a relatively wide prior (i.e. a prior distribution without strong assumptions), a single specimen is sufficient to accurately recover the distribution parameter values.

*Keywords:* Bayesian inference, Bayes' theorem, copula, Gaussian fields, Gaussian processes, Gaussian copula, copula processes, Gaussian copula processes

## 1. Introduction

Explicitly representing the micro-structural grains in predictive models is computationally expensive due to the large number of degrees of freedom required. To omit the explicit representation of the grains in a direct numerical simulation of an RF MEMS, Lucas et al. [1] have developed an approach in which random fields of the effective stiffness tensor are determined, which are used to identify the parameters of a spectral representation [2] that can generate a random field from which the effective material properties random field is obtained by introducing a lower bound and a Cholesky decomposition [1] and possibly a non-Gaussian mapping [3]. Each random field of the effective stiffness tensor forms the input for a single application-scale simulation in which the explicit representation of the grains is omitted (since they are homogenized).

In the framework of Lucas et al. [1], a field of the effective stiffness tensor is determined for each micro-structure by locally probing the micro-structure. This is accomplished by extracting homogenized properties of small-scale statistical volume elements (SVEs) to which a few deformation modes are applied. Many small-scale SVE computations are thus required for a single micro-structure and as many micro-structures must be considered to identify the parameters of the spectral representation, the number of necessary SVE computations is substantial.

*Corresponding author

*Email address:* lars.beex@uni.lu, l.a.a.beex@gmail.com (L.A.A. Beex)

This contribution aims at tackling this problem so that substantially less SVE computations are required, whilst the accuracy remains the same. In contrast to the approach of [1], each field of the effective stiffness tensor is assumed to be a realization from a random field constructed using the copula theorem [4] and Gaussian fields. The questions we aim at answering are thus "how can we describe a random field in a mathematically rigorous way?" and "how can we identify the distribution parameters that govern the random field with a minimum of SVE computations?" The parameters governing the random field based on the copula theorem and Gaussian field are identified using the Bayesian paradigm which may be regarded as a natural way to identify parameters with uncertainty. In this case SVE computations are only necessary to be performed for a single micro-structure, instead of for hundreds of micro-structures.

In order to introduce the proposed methodology relatively gently, we do not focus on a spatial field in two dimensions of the effective stiffness tensor (21 parameters) as [1] have done, but on a spatial field in one dimension of the Young's modulus (one parameter). This can be useful for two dimensional Euler-Bernoulli beams to model slender RF MEMS products in-plane.

To explain our approach of modeling random fields, we first need to discus Gaussian processes (GPs). GPs[1] are well-known and they are elaborately covered in standard text books [5–10]. In the field of mechanics furthermore, GPs have been used in various studies to model data [11–14]. In a GP, the marginal univariate distribution for each data point is a Gaussian distribution (i.e. each observation is a realization from a univariate marginal Gaussian distribution). This assumption is not valid in numerous physical problems. In this contribution for instance, we consider Young's moduli as our observations, which obviously cannot be lower than zero (if a Young's modulus is realized from a Gaussian distribution after all, there is always a possibility that a negative value is generated, no matter how large the mean and how small the standard deviation). A GP can be considered as a generalization of multivariate Gaussian distribution over an infinite dimensional function space [6] (see Subsection 4.1). This entails that a finite dimensional realization of a GP is a realization of a multivariate Gaussian distribution. A generalization of GPs accommodating non-Gaussian features can be accomplished using the copula theorem.

The question is now how we can use the correlation structure of GPs, but include different marginal univariate distributions. To do so, we need to use the concept of copulas. A copula allows one to describe the dependencies between several random variables, regardless of the types of marginal univariate distributions used for the random variables [4]. It accomplishes this by linking the marginal univariate cumulative distribution function (CDF) of each random variable to a single, joint cumulative distribution function. We can also model a multivariate Gaussian distribution using the Gaussian copula [15] and Gaussian univariate distributions as univariate marginal distributions. The Gaussian copula thus merely dictates the correlation structure between the random variables. If one chooses different marginal univariate distributions (instead of the Gaussian one), the resulting joint distribution will have a *Gaussian* correlation structure with *non-Gaussian* univariate marginal distributions. Jaimungal and Ng [16] employed this concept in order to introduce kernel-based copula processes. In [16] kernel functions [5] are used to define the dependency structure of a Gaussian copula. Wilson and Ghahramani [17] presented a general definition for random processes based on the copula theorem, in which the employed copula is not necessarily Gaussian.

Similar to [16] and [17] we use the copula theorem to model our observations (i.e. the field of Young's moduli) as beta-Gaussian copula random fields (i.e. the univariate marginal distributions are beta distributions and the dependency is modeled using a Gaussian copula). In order to identify the parameters of the random field, we use Bayesian inference.

We not only introduce this relatively novel way of modeling random fields to the computational mechanics community, but we also employ Bayesian inference (BI) to identify the random field parameters based on the observations of a single field. The probabilistic framework based on Bayesian inference enables us to quantify the modeling uncertainties as well as identifying the parameters. In the Bayesian paradigm the user's uncertainty about the parameters is described by a probability distribution, which merely describes the user's uncertainty and is not an intrinsic/inherent distribution of the parameters (after all, the random field parameters that we identify are measures for the material randomness). In this paradigm the user's a-priori knowledge and/or assumptions about the unknown parameters, which is represented by the probability distribution, is updated by observations through Bayes' theorem (formula).

The concept of BI is employed to identify parameters in different fields, amongst which in mechanics. One can for instance recognize the works of Isenberg [18], Alvin [19], Beck and Katafygiotis [20], Marwala and Sibusiso [21], Gogu et al. [22], Lai and Ip [23], Daghia et al. [24], Nichols et al. [25] and Gogu et al. [26] for applications in elasticity, the studies of Most [27] and Rappel et al. [14, 28] in elastoplasticity and the studies of studies of Muto and Beck [29], Liu and Au [30], Fitzenz et al. [31], Hernandez et al. [32] and Rappel et al. [33] for other types of history-dependent material descriptions.

[1]Note that in this contribution a random field is a stochastic process that is defined in (Euclidean) space.

Bayesian inference is also employed for the identification of material parameter distributions (material randomness). Rappel and Beex [34] developed a framework based on BI to identify material parameter distributions with a limited number of observations. A similar framework is used by Mohamedou et al. [35] for the identification of the resin's Young's modulus in non-aligned short fiber composites.

Koutsourelakis [36] provided a Bayesian framework to identify spatially varying parameters for perfect plasticity. The framework of [36] is based on a representation of GPs in terms of basis functions [6, 7]. In another study, Koutsourelakis [37] provided a Bayesian framework to identify spatially varying material properties in elasticity. The framework of [37] applies BI directly on the finite element (FE) discretization in which the stiffness tensor (i.e the spatially varying properties) over each element is constant. These constant tensors over each element appear in the posterior as parameters to be inferred (i.e. the dimensions of the posterior equal the number of FEs). Uribe et al. [38] employed Bayesian inference for the identification of a hydraulic conductivity field, which research is represented as a GP with a Karhunen-Loève expansion. Furthermore, Vigliotti et al. [39] recently employed Bayesian inference to identify spatial (non-random) fields of Young's moduli and Poisson's ratios. In their work, the spatial fields are constructed using B-splines and model selection based on BI was employed to identify the order of the B-splines.

The outline of this paper is as follows. Section 2 discusses the concept of this study in more detail from a mechanics point of view. In Section 3 a general description of Bayesian inference is provided. In Section 4, we discuss the construction and identification of our random fields in detail. In Section 5 we present our results. Finally, we offer our conclusions in Section 6.

## 2. General concept of the study

In this short section, we discuss the general concept of our study in slightly more detail. The discussion here is based on the illustration in Fig. 1. On the left, we can observe $n_b$ columnar micro-structures, which are all realizations of the same RF MEMS. Elastic simulations of these polycrystalline columnar micro-structures (e.g. to determine the distribution of resonance frequencies) are computationally costly because each grain requires to be discretized with numerous FEs.

Alternatively, one could model them with beam elements if random fields of effective material parameters can be generated. Although we do not perform the actual beam simulations, we refer the reader again to [1] for more detailed information. The results of [1] only show small differences between the homogenized and direct numerical simulations as long as the spatial correlation is correctly captured, which requires to use stochastic finite elements of size lower than the latter.

In order to generate random fields of effective Young's moduli, we first need a mathematically rigorous way to model the random fields. Subsequently, we need to identify the parameters that govern the random fields. For the identification, we first need measurements of the fields of effective Young's moduli. For this purpose, 10 statistical volume elements (SVEs) are extracted from each micro-structure, which are numerically deformed (second column from the left in Fig. 1). The results of these SVE computations are fields of 10 effective Young's moduli in space per polycrystalline realization (third column from the left in Fig. 1).

In [1], many micro-structures were required to train a spectral field generator. In the current work, the random fields are considered as realizations of a stochastic process/field (beta-Gaussian copula process, $\pi(\mathbf{p}|\mathbf{z})$ in Fig. 1) *and* BI is used (1) as a natural way to identify parameters with uncertainty, and (2) to ensure that the identification can be based on a limited number of observations (i.e. a single polycrystalline realization is sufficient). In order to verify that the characterized random field generates similar fields of Young's moduli, we finally compare the generated realizations of our model to the $n_b - 1$ validation realizations (see Fig. 1).

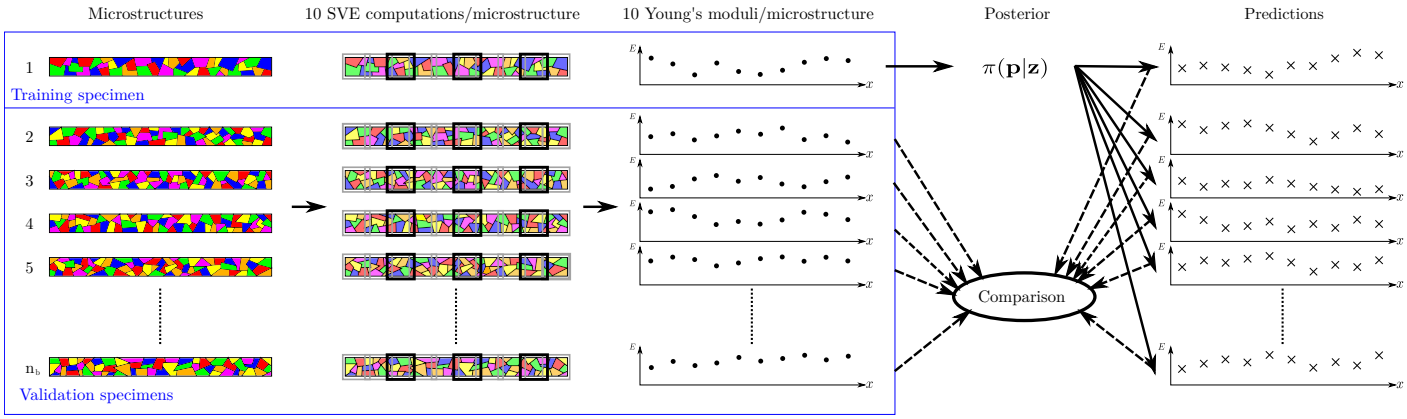


Figure 1: Illustration of the general concept of the study.

## 3. Bayesian inference

Bayesian inference is a probabilistic framework that fits a probability model to a set of observations. The results of the inference are summarized as a probability distribution in terms of the parameters of the probability model (i.e. the model of the observations) and a probability distribution for unobserved quantities such as new observations [7]. The employed probability distributions in this approach address the uncertainties. In this framework furthermore, the probability distribution that represents the user's initial belief (about a parameter or model) is updated with the information of the measurements according to Bayes' rule [7].

Let $\mathbf{z} = \begin{bmatrix} z_1 & \cdots & z_{n_o} \end{bmatrix}^T$ be the vector of $n_o$ observations and $\mathbf{p}$ the vector of $n_p$ parameters of the mathematical model to describe our observations. According to Bayes' formula we have:

$$\pi(\mathbf{p}|\mathbf{z}) = \frac{\pi(\mathbf{p})\pi(\mathbf{z}|\mathbf{p})}{\pi(\mathbf{z})} = \frac{1}{\zeta}\pi(\mathbf{p})\pi(\mathbf{z}|\mathbf{p}). \tag{1}$$

In this equation $\pi(\mathbf{p})$ denotes the prior PDF (i.e. the PDF that represents one's assumed prior knowledge about the parameters, e.g. the fact that the Young's modulus cannot be negative), $\pi(\mathbf{z}|\mathbf{p})$ denotes the likelihood function (i.e. the PDF that measures the likelihood of observations $\mathbf{z}$, for a given set of parameter values $\mathbf{p}$), $\pi(\mathbf{p}|\mathbf{z})$ denotes the posterior PDF (i.e. the PDF that describes the plausibility of parameter set $\mathbf{p}$, for the given set of observations, $\mathbf{z}$) and $\pi(\mathbf{z})$ is called evidence. Since the values for vector $\mathbf{z}$ are known, the evidence is a constant number ($\pi(\mathbf{z}) = \zeta \in \mathbb{R}^+$) which is thus independent of the parameters (i.e. the variables of interest). In other words it suffices to write Eq. (1) as follows:

$$\pi(\mathbf{p}|\mathbf{z}) \propto \pi(\mathbf{p})\pi(\mathbf{z}|\mathbf{p}). \tag{2}$$

Note that the statistical summaries of the posterior, such as the mean, the MAP (i.e. the 'maximum-a-posteriori-probability' or the parameter values at which the posterior is maximal) and the covariance matrix (i.e. the matrix that measures the correlation between the parameters), are independent of scaling factor $\frac{1}{\zeta}$.

In order to calculate the statistical summaries, numerical frameworks are generally required. Markov chain Monte Carlo (MCMC) techniques [40] are frequently employed to draw samples from the posterior PDF. The drawn samples can be used to approximate statistical summaries and predict new observations. Readers are referred to [28, 41] for more details.

## 4. Construction of the random fields and their identification

In order to model random parameter fields, it is essential to first discuss the Gaussian processes and the copula theorem. Finally we introduce the Gaussian copula processes concept, their formulation and their identification based on BI (see Section 3). Note that random fields are the same as stochastic processes which take spatial variables as their index (input) set. Below, we stick to the term *process* to explain the basic concepts.

*4.1. Gaussian processes*

In this subsection a practical description of Gaussian processes is presented. Readers who are interested in more details are referred to [5]. Rasmussen [42] defines a Gaussian process as a collection of an infinite number of random variables, which has a Gaussian joint distribution for any subset of these random variables. In other words, a Gaussian process is an extension of a multivariate Gaussian distribution to an infinite dimensional Gaussian distribution [7].

A Gaussian process is fully characterized by its mean function $m(x)$ and covariance function $k(x, x')$. Note that $x$ and $x'$ are inputs (here, the spatial coordinates). Now one can write:

$$f(x) \sim \mathrm{GP}(m(x), k(x, x')). \tag{3}$$

Note that the mean function $m(x)$ is in fact the mean of the function $f(x)$, i.e. $\mathbb{E}[f(x)]$, at point $x$. $k(x, x')$ specifies the covariance of the process at two points $x$ and $x'$, i.e. $\mathbb{E}[(f(x) - m(x))(f(x') - m(x'))]$. For a finite set of points we have:

$$\mathbf{f} \sim N(\mathbf{m}, \mathbf{K}), \tag{4}$$

where $\mathbf{m} = \begin{bmatrix} m(x_1) & \cdots & m(x_n) \end{bmatrix}^T$, $K_{ij} = k(x_i, x_j)$ and $\mathbf{f} = \begin{bmatrix} f(x_1) & \cdots & f(x_n) \end{bmatrix}^T$.

Often, as in our study, the assumption $m(x) = 0$ is used [10]. A frequently chosen covariance function is the squared exponential covariance function:

$$k(x, x') = \lambda^2 \exp\Big( - \frac{(x - x')^2}{2\psi^2} \Big), \tag{5}$$

where $\lambda$ controls the magnitude and $\psi$ the smoothness of the function. As $x$ is defined in space for us, $\psi$ is a length scale parameter in our work. Note that if a Gaussian process is used for regression (or modeling) $\lambda$ and $\psi$ are unknown parameters that should be identified. In this study we set $\lambda$ equal to 1.

The concepts given in this subsection will be used in Subsection 4.3 to construct the Gaussian copula processes.

*4.2. Copulas*

A copula is defined as a function that joins one dimensional marginal distributions to their multivariate distribution [4]. Using copulas one can model the dependencies between several random variables. In the next subsection we will use this feature in combination with the correlation structure of Gaussian processes to construct Gaussian copula processes. In the current subsection, we elaborate on copulas.

Let $\mathbf{P} = \begin{bmatrix} P_1 & \cdots & P_{n_p} \end{bmatrix}^T$ be a vector of $n_p$ random variables with joint cumulative distribution function (CDF) $\Pi$ and $\Pi_i$ be the marginal univariate CDF for each random variable. Sklar's theorem [43] states that an n-dimensional copula $C$ exists such that:

$$\Pi(p_1, \cdots, p_{n_p}) = C(\Pi_1(p_1), \cdots, \Pi_{n_p}(p_{n_p})). \tag{6}$$

The equation above can be used to obtain the joint PDF as follows:

$$\pi(p_1, \cdots, p_{n_p}) = c(\Pi_1(p_1), \cdots, \Pi_{n_p}(p_{n_p})) \prod_{i=1}^{n_p} \pi_i(p_i), \tag{7}$$

where $c(u_1, \cdots, u_{n_p}) = \frac{\partial C(u_1, \cdots, u_{n_p})}{\partial u_1 \cdots \partial u_{n_p}}$ with $u_i = \Pi_i(p_i)$ and $\pi_i(p_i)$ denotes the $i^{\text{th}}$ marginal PDF.

Various types of copulas exist to model dependencies between random variables, see e.g. [44]. Since we base our work on GPs to create copula processes however, we restrict ourselves to the Gaussian copula [15]. The density of a Gaussian copula is written as [15]:

$$c(\mathbf{u}|\mathbf{\Gamma}_C) = \frac{1}{\sqrt{|\mathbf{\Gamma}_C|}} \exp\Big( - \frac{1}{2} \begin{bmatrix} \Phi^{-1}(u_1) & \cdots & \Phi^{-1}(u_{n_p}) \end{bmatrix} \times (\mathbf{\Gamma}_C^{-1} - \mathbf{I}) \times \begin{bmatrix} \Phi^{-1}(u_1) & \cdots & \Phi^{-1}(u_{n_p}) \end{bmatrix}^T \Big), \tag{8}$$

where $u_i = \Pi_i(p_i)$, $\mathbf{\Gamma}_C \in [-1, 1]^{n_p \times n_p}$ denotes the covariance matrix containing the Pearson correlation coefficient (i.e. Pearson's $\rho$ a measure for the linear relationship between two random variables, see e.g. [45]), $\Phi(\tilde{p})$ denotes the standard Gaussian CDF (i.e. $\tilde{p} \sim N(0, 1) = \frac{1}{\sqrt{2\pi}} \exp(-\frac{\tilde{p}^2}{2})$), $|\cdot|$ denotes the determinant and $\mathbf{I}$ the $n_p \times n_p$ identity matrix. Substituting the Gaussian copula density given in Eq. (8) and selected univariate marginal PDFs in Eq. (7) one can construct the multivariate PDF for modeling the data. In the next subsection we will combine the concept of copulas with Gaussian processes in order to explain Gaussian copula processes.

*4.3. Gaussian copula processes*

In this subsection we discuss the basic idea of Gaussian copula processes. In other words, here we describe the construction of the random fields characterized by non-Gaussian univariate marginal distributions that are joined in a single distribution using Gaussian copulas. We actually use beta distributions for the univariate marginal distributions.

The advantage of this approach is that samples can still be generated from GPs (multivariate Gaussian distributions in practice), which are then, via the CDF of the univariate Gaussian distribution and the inverse CDF of the beta distribution, transformed to samples generated from the new random field (which is governed by univariate, marginal beta distributions coupled with Gaussian copulas). A pseudo-algorithm to generate a sample from a beta-Gaussian copula distribution process is presented below.

**Algorithm 1** Pseudo-algorithm to generate a sample from a beta-Gaussian

1: Generate a sample from GP with given covariance function (in practice the sample is generated from a multivariate Gaussian distribution with given covariance matrix)
2: Transform each of the values in line 1 through a univariate Gaussian CDF to a uniformly distributed value.
3: Transform the values in line 2 through a inverse beta CDF.

Note that the pseudo-algorithm presented here can also be used to generate samples from stochastic processes with other types of univariate marginal PDFs/CDFs. The only requirement is that the CDF (and its inverse) must be changed.

*4.3.1. Formulation and identification of the Gaussian copula process*

Let $\mathbf{z}$ again be the vector of our $n_o$ observations of the Young's modulus. Our goal is to model these observations using the beta-Gaussian copula process. This means that we assume the univariate marginal distributions to be four-parameter beta distributions:

$$\pi(E) = \frac{(E-a_1)^{\alpha-1}(a_2-E)^{\beta-1}}{(a_2-a_1)^{\alpha+\beta-1}B(\alpha,\beta)}, \tag{9}$$

where $E$ denotes the Young's modulus, $\alpha$ and $\beta$ denote the shape parameters of the univariate PDF, $a_1$ and $a_2$ denote the lower and upper bounds, respectively and $B(\cdot,\cdot)$ denotes the beta function.

We model the dependency structure using the Gaussian copula for which the correlation matrix components (see Eq. (8)) are computed as:

$$(\Gamma_C)_{ij} = \exp\big(-\frac{(x_i-x_j)^2}{2\psi^2}\big), \tag{10}$$

where $x_i$ and $x_j$ denote two locations (which may be the same). The parameters that we need to identify are $\alpha$, $\beta$ and $\psi$, since bounds $a_1$ and $a_2$ are known for a given crystal structure. Rewriting the Bayesian formula for these three parameters (see Eq. (2)) we obtain:

$$\pi(\alpha,\beta,\psi|\mathbf{z}) \propto \pi(\alpha)\pi(\beta)\pi(\psi)\pi(\mathbf{z}|\alpha,\beta,\psi), \tag{11}$$

where $\pi(\alpha)$, $\pi(\beta)$ and $\pi(\psi)$ together form uncorrelated prior $\pi(\alpha,\beta,\phi) = \pi(\alpha)\pi(\beta)\pi(\phi)$ and $\pi(\mathbf{z}|\alpha,\beta,\psi)$ denotes the likelihood. Based on the assumption that the observations for a single polycrystalline bar are a realization from a beta-Gaussian copula process, the likelihood function reads:

$$\pi(\mathbf{z}|\alpha,\beta,\psi) = c(u_{\mathbf{z}}|\mathbf{\Gamma}_C)\prod_{i=1}^{n_o}\pi(z_i), \tag{12}$$

where $c(u_{\mathbf{z}})$ is given in Eq. (8), $\pi(z_i)$ is given in Eq. (9) and $u_{z_i}$ is the value of the four parameter beta CDF at $z_i$.

## 5. Results

This section presents the results for the identification of the beta-Gaussian copula process to the model the random fields of effective Young's moduli. The results are compared to the validation results of Fig. 1 in order to show how similar the identified random fields are to the real ones.

*5.1. Identification of the beta-Gaussian copula process parameters*

In this subsection we employ the identification procedure to identify the parameters of the beta-Gaussian process that models our observations. We consider a columnar polysilicon micro-structure of average grain diameter of 0.2 $\mu$m and of random grain orientation making the homogenized properties in-plane isotropic. The set of observations are 10 evenly distanced Young's moduli (their distance is 0.2 $\mu$m) that are computed by homogenization of 10 SVE which are 0.4 $\mu$m long (in the direction in which the sampling is performed) and 0.5 $\mu$m wide.

For the identification, we first construct our priors (i.e. $\pi(\alpha)$, $\pi(\beta)$ and $\pi(\psi)$ in Eq.(11)). Note that since we have a clear knowledge about the bounds of the Young's modulus (i.e. $a_1$ and $a_2$ in Eq. (9)), they do not appear in our inference as unknowns (see Eq. (11)). We choose the following priors for the shape parameters of the beta distribution (i.e. $\alpha$ and $\beta$):

$$\pi(p_{\text{uni}}) \propto \begin{cases} \exp\Big( - \frac{(p_{\text{uni}} - \overline{p_{\text{uni}}}^{\text{prior}})^2}{2 s_{p_{\text{uni}}}^{\text{prior}\,2}} \Big) & \text{if } p_{\text{uni}} \geq 0 \\ 0 & \text{otherwise} \end{cases}, \tag{13}$$

where $p_{\text{uni}}$ refers either to $\alpha$ or $\beta$, $\overline{p_{\text{uni}}}^{\text{prior}}$ denotes the prior mean value and $s_{p_{\text{uni}}}^{\text{prior}}$ denotes the prior standard deviation. Note that the shape parameters of a beta distribution can not be lower than zero, which is explicitly incorporated in our prior. The chosen values are reported in Table 1. Note that we have chosen $\overline{\alpha}^{\text{prior}}$ and $\overline{\beta}^{\text{prior}}$ based on the mean value and standard deviation of the observations (having mean value and standard deviation of our observations we can get a rough estimation for $\overline{\alpha}^{\text{prior}}$ and $\overline{\beta}^{\text{prior}}$). The prior for $\psi$ is furthermore chosen to be a uniform distribution between 0.2 $\mu$m and 3.2 $\mu$m. This minimum is used as it is unphysical to consider a length scale parameter lower than the minimum distance between two Young's modulus sampling points. The maximum is used as we assume that the length scale parameter will not be larger than the bar.

Table 1: The chosen values for the parameters that define our priors.

| | | | |
|---|---|---|---|
| $\overline{\alpha}^{\text{prior}}$ | 19.9829 | $a_1$ (GPa) | 130 |
| $s_{\alpha}^{\text{prior}}$ | 9.9915 | $a_2$ (GPa) | 188 |
| $\overline{\beta}^{\text{prior}}$ | 18.7793 | [2]$\psi_{\text{low}}$ ($\mu$m) | 0.2 |
| $s_{\alpha}^{\text{prior}}$ | 9.3896 | $\psi_{\text{up}}$ ($\mu$m) | 3.2 |

We use the adaptive Metropolis method [46] to draw samples from the posterior and hence, to obtain the statistical summaries such as the MAP. $500 \times 10^3$ are drawn from the posterior whilst burning the first 30% of the samples. The statistical summaries are reported in Table 2 and Eq. (14). $\mathbf{\Gamma}^{\text{posterior}}$ denotes the numerically approximated covariance matrix of the posterior.

Table 2: The statistical summaries of identified posteriors

| $\alpha$ | $\beta$ | $\psi$ ($\mu$m) |
|---|---|---|
| MAP estimates | | |
| 18.1184 | 17.9530 | $2.0002 \times 10^{-1}$ |
| Mean values | | |
| 17.5591 | 17.3137 | 0.2171 |

$$\mathbf{\Gamma}^{\text{posterior}} = \begin{bmatrix} 28.1458 & 23.7931 & -0.022 \\ & 26.9678 & -0.0209 \\ \text{symmetric} & & 1.5817 \times 10^{-4} \end{bmatrix}. \tag{14}$$

The marginal posteriors as well as some realizations of the identified beta-Gaussian process are shown in Fig. 2. It is important to note that here we are not using the beta-Gaussian copula process to perform a *regression* but the idea is to identify the parameters of the beta-Gaussian copula process from which our (and new) observations are

[2]Lower and upper bounds for the uniform distribution which is assigned as prior for $\psi$.

drawn. Any realization of this beta-Gaussian copula process is thus a field of Young's moduli. Furthermore, in this figure we have presented the observations as well as two verification sets. Note that the verification points are not used in the identification procedure. At first sight, it indeed seems that the identified beta-Gaussian copula process can generate fields that are similar to our observations and verification point sets.

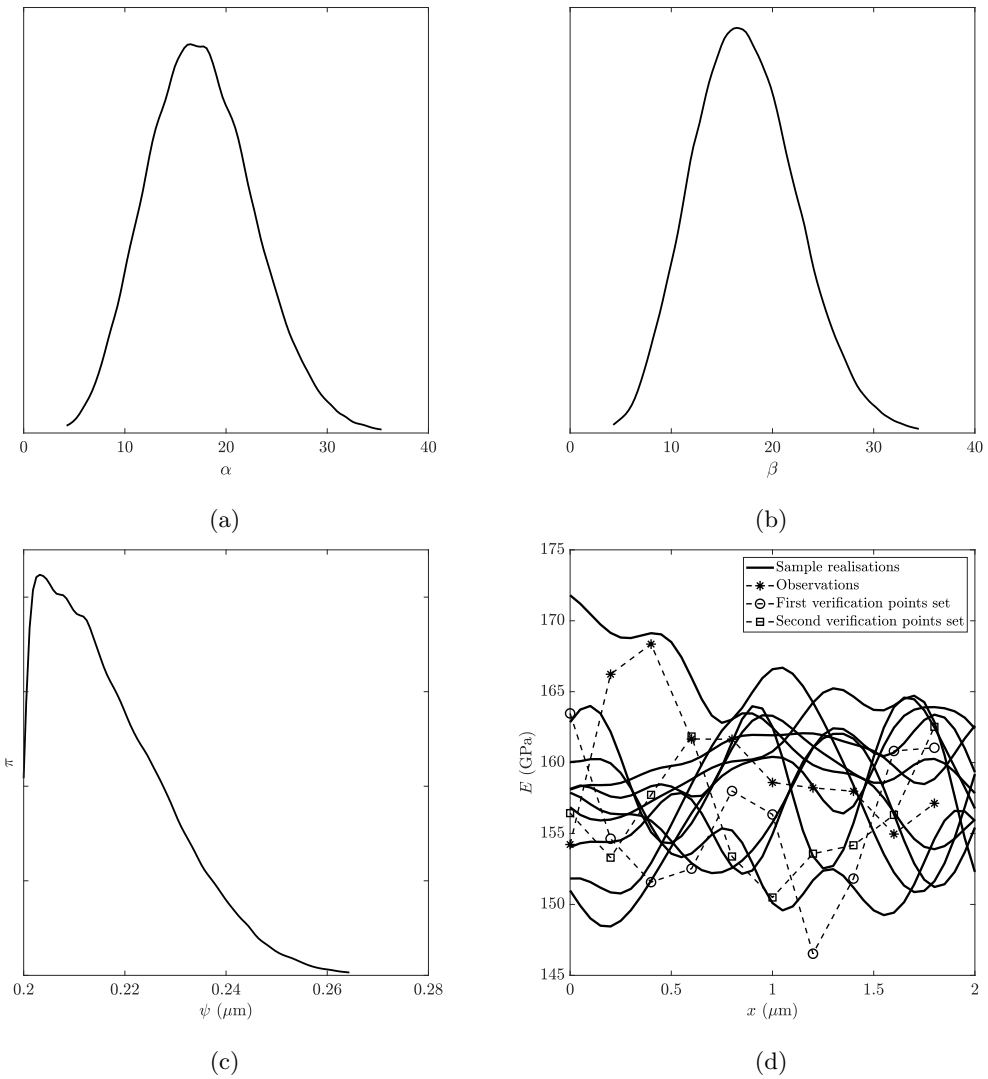


Figure 2: Marginal posteriors, some realizations from the identified process, observations and two verification fields. (a) $\alpha$, (b) $\beta$, (c) $\psi$ and (d) samples realization from the identified process. The marginal probability density functions are not normalized. Note that the verification points are not used in the identification process. Once the parameters are inferred, random fields can be generated for more locations than the 10 that we have considered, as we have done for the sample realizations in (d).

### *5.2. Performance of the beta-Gaussian process modeling approach*

In this section we check the performance of our modeling and identification approach more rigorously. This is achieved by comparing our model outputs with 417 fields of 10 Young's moduli which are obtained through the SVE computations. These fields are not used in the identification procedure. Note that we only focus on accuracy and not on computational performance. The reason for this is that we only focus on a single field of 10 Young's moduli and the MCMC approach has to be employed only once. This is negligible compared to the empirical approach of [1].

First, we compare the univariate marginal distributions of our modeling framework with the univariate marginal distribution of SVE computations. Fig. 3(a) shows both the simulated and the SVE computations' univariate distributions. The simulated results in Fig. 3(a) were created using the following steps:

(1) draw a sample for $\alpha$ and $\beta$ from the posterior (Fig. 2, these are available through MCMC),

(2) use the values of the previous step to draw 4170 Young's moduli from the corresponding beta distribution and plot the histogram,

(3) repeat the previous steps 50 times.

A comparison of the SVE computations' univariate marginal distribution and the distribution corresponding to the mean values of $\alpha$ and $\beta$ is presented in Fig. 3(b). The univariate marginal distributions based on parameter values in 95% credible region (i.e. the region that contains 95% of the posterior [28]) are also presented in this figure. The graphical test in [7] shows that the modeling approach in this contribution generates samples that are in a reasonable agreement.

Although we have chosen beta distribution as univariate marginal distributions, Fig. 3 shows that the univariate marginal distributions are similar to Gaussian distributions. Apparently, these polycrystalline microstructures probabilistically behave in Gaussian manner, although the beta distribution does intrinsically include bounds (given in Table 1).

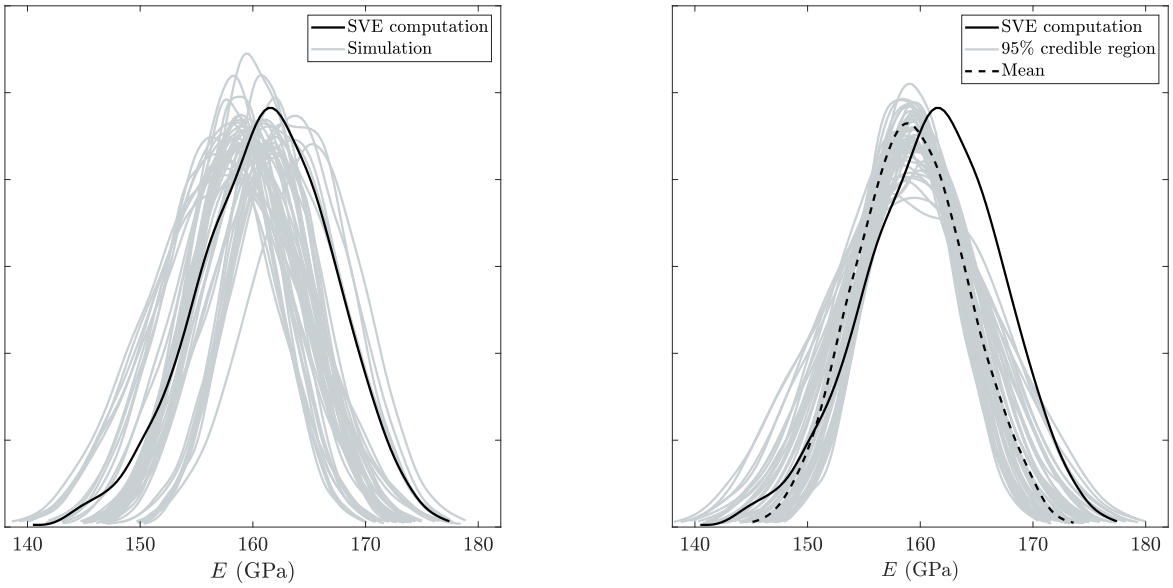


Figure 3: Comparison of univariate marginal distributions (a) SVE computations and simulated univariate distributions and (b) SVE computations, univariate marginal distribution based on the mean of the posterior and univariate marginal distributions based on parameter values in the 95% credible region (i.e. the region that contains 95% of the posterior [28]). This graphical test [7] shows a reasonable agreement between our modeling and test data.

Next, we compare the correlation matrix of our validation sets with the ones from our modeling approach. Our goal is to see if the realizations of our modeling approach have similar correlation coefficients as our validation sets (417 fields of 10 Young' moduli in each field). In order to perform the comparison, we use the MCMC samples of $\psi$ (i.e. the samples that approximate the posterior, see Fig. 2(c)) to create many possible correlation matrices. Next we draw 417 10-dimensional realizations from a Gaussian distribution with zero mean and the covariance matrix constructed with the identified value for $\phi$ (the 10-dimensional Gaussian distribution is a marginalization of GP). Now we can calculate the Pearson correlation coefficients of 417 realizations for each MCMC sample. It is important to note that we can *not* directly compare the correlation matrices that each MCMC (posterior) sample creates (i.e. we can not directly compare the first correlation matrix). This is due to the fact that the samples from any distribution represent the true characteristic values (e.g. mean, variance, correlation coefficients,...) if the number of samples is infinite (or large enough). Fig. 4 shows the resulting distributions for correlation coefficients as well as the validation correlation coefficients. Note that the correlation matrix is symmetric and all its diagonal components equal to 1. We therefore do not compare those ones. One can see that all the PDFs resulting from our modeling approach contain the correlation coefficient of the entire validation sets (dashed line). Eq. (15) furthermore shows the spatial position of the correlation coefficients. $\Delta x = 0.2$ $\mu$m and $x_0$ denotes the location of the first component of our 10 Young's moduli field.

It is important to note that from a probabilistic perspective, the distributions in Fig. 4 show the plausible values for the correlation coefficients. In an ideal case, we would like all dashed lines to be close to the center, because the closer an observation is to center, the more plausible the observation. Although not all dashed lines are in the center of the distributions of Fig. 4, they are clearly well inside the distributions. This means that our framework is able to predict the observations.

$$
\begin{array}{c|cccccccccc}
\text{location} & x_0 & x_0{+}\Delta x & x_0{+}2\Delta x & x_0{+}3\Delta x & x_0{+}4\Delta x & x_0{+}5\Delta x & x_0{+}6\Delta x & x_0{+}7\Delta x & x_0{+}8\Delta x & x_0{+}9\Delta x \\
x_0 & 1 & \rho_{12} & \rho_{13} & \rho_{14} & \rho_{15} & \rho_{16} & \rho_{17} & \rho_{18} & \rho_{19} & \rho_{110} \\
x_0{+}\Delta x & & 1 & \rho_{23} & \rho_{24} & \rho_{25} & \rho_{26} & \rho_{27} & \rho_{28} & \rho_{29} & \rho_{210} \\
x_0{+}2\Delta x & & & \ddots & \rho_{34} & \rho_{35} & \rho_{36} & \rho_{37} & \rho_{38} & \rho_{39} & \rho_{310} \\
x_0{+}3\Delta x & & & & \ddots & \rho_{45} & \rho_{46} & \rho_{47} & \rho_{48} & \rho_{49} & \rho_{410} \\
x_0{+}4\Delta x & & & & & \ddots & \rho_{56} & \rho_{57} & \rho_{58} & \rho_{59} & \rho_{510} \\
x_0{+}5\Delta x & & & & \text{symmetric} & & \ddots & \rho_{67} & \rho_{68} & \rho_{69} & \rho_{610} \\
x_0{+}6\Delta x & & & & & & & \ddots & \rho_{78} & \rho_{79} & \rho_{710} \\
x_0{+}7\Delta x & & & & & & & & \ddots & \rho_{89} & \rho_{810} \\
x_0{+}8\Delta x & & & & & & & & & 1 & \rho_{910} \\
x_0{+}9\Delta x & & & & & & & & & & 1
\end{array}
. \tag{15}
$$

## 6. Conclusions

In this contribution, a framework based on Gaussian fields, the copula theorem and Bayesian inference is proposed to model and identify random fields of Young's moduli. One field of Young's moduli was sufficient to identify the random field parameters.

Gaussian fields are widely used in various researches and are well covered in standard text books. However, the assumption of the Gaussian distribution for the univariate marginal distribution in Gaussian fields is often not valid to model random parameter fields, as many material parameters have well-defined physical bounds. We therefore propose a framework that combines Gaussian fields with the copula theorem. This framework allows us to create random fields with a Gaussian correlation structure and non-Gaussian univariate marginal distributions. Its advantage is that each field can be generated using Gaussian fields, but then, via two standard transformations, is morphed in a new field that originates from a Gaussian correlation structure and non-Gaussian univariate marginal distributions.

To identify the parameters of the aforementioned random field we use Bayesian inference as a natural way of identifying parameters with uncertainty. Moreover, Bayesian inference allows the identification to be performed with a considerably small number of observations (a set of 10 Young's moduli).

To validate the accuracy of the modeled random fields and the identification of its parameters, we have compared the marginal univariate distributions and correlation coefficients that our framework produces with the ones of 417 validation sets, which were not used in the identification procedure. Our results show that the univariate marginal distributions of the identified random fields are in good agreement with the univariate marginal distribution of the validation sets. The results on the correlation coefficients show that the distributions of correlation coefficients include the values of our validation sets. The probabilistic nature of the framework proposed in this contribution enables us to predict the validation sets' correlation coefficients and univariate marginal distributions as a plausible value in our modeling.

The framework presented in this contribution is used to model scalar fields, i.e. the field of a single material parameter. However, it is possible that one is interested in multi-output or vector fields, i.e. fields of more than one type of material parameters. If the parameters of interest are independent, the proposed framework can directly be applied (separately for each type of material parameter). If the types of parameters are on the other hand dependent on each other, the correlation structure between the different types must be modeled (in addition to the spatial correlation as considered in the current contribution). We aim to treat this issue in a future contribution.

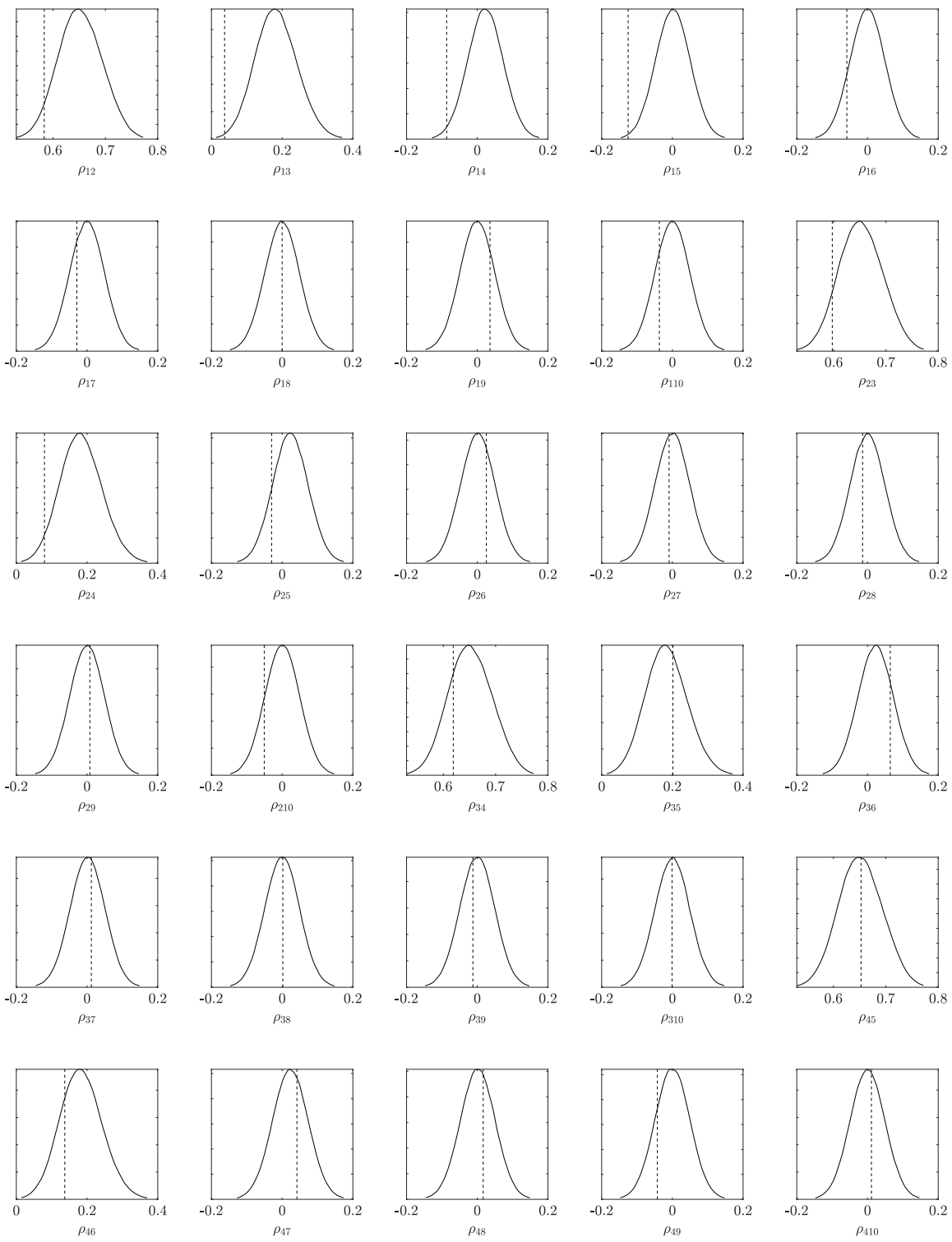


Figure 4: The correlation coefficients' distributions and the correlation coefficients of the validation sets (dashed line). The distributions for the correlation coefficients are obtained using the MCMC samples which approximate the posterior. One can see that all the distributions include the validation sets' correlation coefficients. This entails that the fields generated by the framework have similar correlation coefficients to those of the validation sets. Eq. (15) shows the spatial position of the correlation coefficients. $\Delta x = 0.2$ $\mu$m and $x_0$ is the spatial position of the first component of our 10 Young's moduli set.

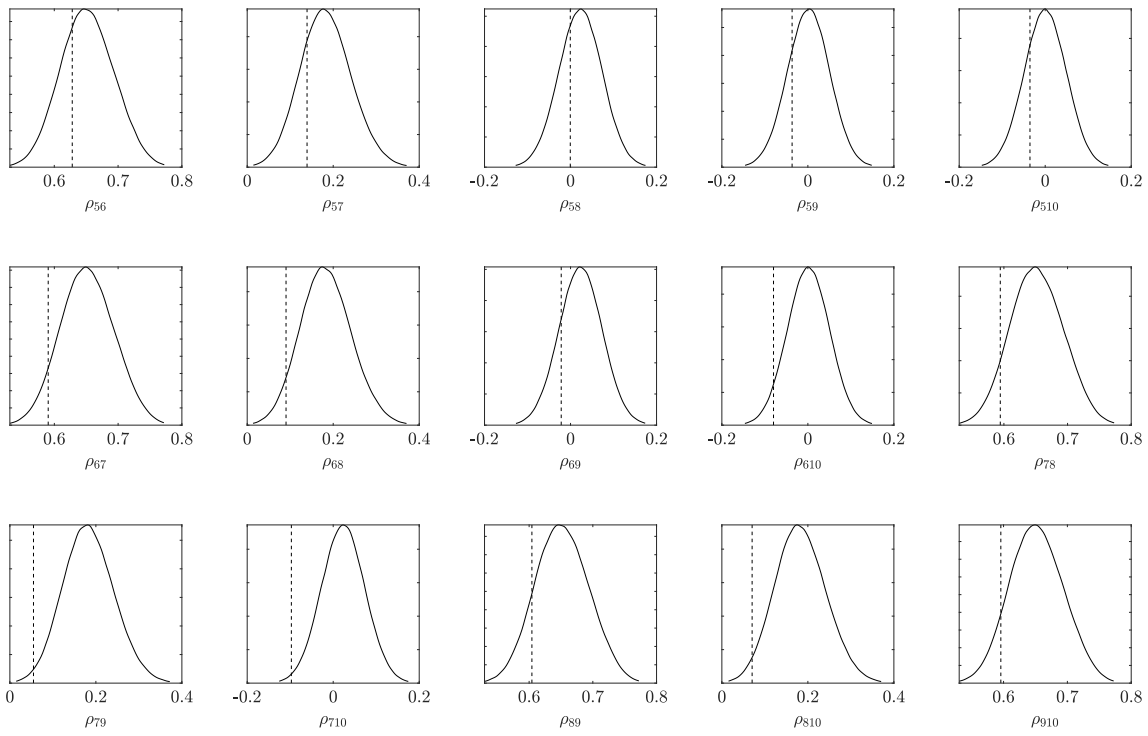


Continued Figure 4: The correlation coefficients' distributions and the correlation coefficients of the validation sets (dashed line). The distributions for the correlation coefficients are obtained using the MCMC samples which approximate the posterior. One can see that all the distributions include the validation sets' correlation coefficients. This entails that the fields generated by the framework have similar correlation coefficients to those of the validation sets. Eq. (15) shows the spatial position of the correlation coefficients. $\Delta x = 0.2$ $\mu$m and $x_0$ is the spatial position of the first component of our 10 Young's moduli set.

**Acknowledgements**

Hussein Rappel and Lars Beex gratefully acknowledge the financial support of the Fonds National de la Recherche Luxembourg under grant number INTER/DFG/16/11501927.

**References**

[1] V. Lucas, J. C. Golinval, S. Paquay, V. D. Nguyen, L. Noels, L. Wu, A stochastic computational multiscale approach: Application to MEMS resonators, Computer Methods in Applied Mechanics and Engineering 294 (2015) 141–167.

[2] M. Shinozuka, C. M. Jan, Digital simulation of random processes and its applications, Journal of Sound and Vibration 25 (1) (1972) 111–128.

[3] L. Wu, V. Lucas, V. D. Nguyen, J. C. Golinval, S. Paquay, L. Noels, A stochastic multi-scale approach for the modeling of thermo-elastic damping in micro-resonators, Computer Methods in Applied Mechanics and Engineering 310 (2016) 802–839.

[4] R. B. Nelsen, An introduction to copulas, Springer Science & Business Media, 2007.

[5] C. E. Rasmussen, C. K. I. Williams, Gaussian processes for machine learning, Vol. 1, MIT press Cambridge, 2006.

[6] D. J. C. MacKay, Information theory, inference and learning algorithms, Cambridge university press, 2003.

[7] A. Gelman, J. B. Carlin, H. S. Stern, D. B. Rubin, Bayesian data analysis, Chapman & Hall/CRC Texts in Statistical Science, Chapman & Hall/CRC, 2003.

[8] C. M. Bishop, Pattern recognition and machine learning, Information Science and Statistics, Springer Science & Business Media, 2006.

[9] S. Rogers, M. Girolami, A first course in machine learning, second edition, 2nd Edition, Chapman & Hall/CRC, 2016.

[10] K. P. Murphy, F. Bach, Machine learning: A probabilistic perspective, Adaptive Computation and Machine Learning series, MIT press Cambridge, 2012.

[11] M. C. Kennedy, A. O'Hagan, Bayesian calibration of computer models, Journal of the Royal Statistical Society: Series B (Statistical Methodology) 63 (3) (2001) 425–464.

[12] M. J. Bayarri, J. O. Berger, R. Paulo, J. Sacks, J. A. Cafeo, J. Cavendish, C. H. Lin, J. Tu, A framework for validation of computer models, Technometrics 49 (2) (2007) 138–154. arXiv:https://doi.org/10.1198/004017007000000092.

[13] P. D. Arendt, D. W. Apley, W. Chen, Quantification of model uncertainty: Calibration, model discrepancy, and identifiability, Journal of Mechanical Design 134 (10) (2012) 100908.

[14] H. Rappel, L. A. A. Beex, L. Noels, S. P. A. Bordas, Identifying elastoplastic parameters with Bayes' theorem considering output error, input error and model uncertainty, Probabilistic Engineering Mechanics 55 (2018) 28–41.

[15] P. X. Song, Multivariate dispersion models generated from Gaussian copula, Scandinavian Journal of Statistics 27 (2) (2000) 305–320.

[16] S. Jaimungal, E. K. H. Ng, Kernel based copula processes, in: W. Buntine, M. Grobelnik, D. Mladenić, J. Shawe-Taylor (Eds.), Machine Learning and Knowledge Discovery in Databases, Springer Science & Business Media, Berlin, Heidelberg, 2009, pp. 628–643.

[17] A. G. Wilson, Z. Ghahramani, Copula processes, in: Advances in Neural Information Processing Systems, 2010, pp. 2460–2468.

[18] J. Isenberg, Progressing from least squares to Bayesian estimation, in: Proceedings of the 1979 ASME design engineering technical conference, New York, 1979, pp. 1–11.

[19] K. F. Alvin, Finite element model update via bayesian estimation and minimization of dynamic residuals, AIAA journal 35 (5) (1997) 879–886.

[20] J. L. Beck, L. S. Katafygiotis, Updating models and their uncertainties. I: Bayesian statistical framework, Journal of Engineering Mechanics 124 (4) (1998) 455–461.

[21] T. Marwala, S. Sibisi, Finite element model updating using Bayesian framework and modal properties, Journal of Aircraft 42 (1) (2005) 275–278.

[22] C. Gogu, R. Haftka, R. Le Riche, J. Molimard, A. Vautrin, Introduction to the Bayesian approach applied to elastic constants identification, AIAA journal 48 (5) (2010) 893–903.

[23] T. C. Lai, K. H. Ip, Parameter estimation of orthotropic plates by Bayesian sensitivity analysis, Composite Structures 34 (1) (1996) 29–42.

[24] F. Daghia, S. de Miranda, F. Ubertini, E. Viola, Estimation of elastic constants of thick laminated plates within a Bayesian framework, Composite Structures 80 (3) (2007) 461–473.

[25] J. M. Nichols, W. A. Link, K. D. Murphy, C. C. Olson, A bayesian approach to identifying structural nonlinearity using free-decay response: Application to damage detection in composites, Journal of Sound and Vibration 329 (15) (2010) 2995–3007.

[26] C. Gogu, W. Yin, R. Haftka, P. Ifju, J. Molimard, R. Le Riche, A. Vautrin, Bayesian identification of elastic constants in multi-directional laminate from moiré interferometry displacement fields, Experimental Mechanics 53 (4) (2013) 635–648.

[27] T. Most, Identification of the parameters of complex constitutive models: Least squares minimization vs. Bayesian updating, in: D. Straub (Ed.), Reliability and optimization of structural systems, CRC press, 2010, pp. 119–130.

[28] H. Rappel, L. A. A. Beex, J. S. Hale, L. Noels, S. P. A. Bordas, A tutorial on bayesian inference to identify material parameters in solid mechanics, Archives of Computational Methods in Engineering`doi: 10.1007/s11831-018-09311-x`.

[29] M. Muto, J. L. Beck, Bayesian updating and model class selection for hysteretic structural models using stochastic simulation, Journal of Vibration and Control 14 (1-2) (2008) 7–34.

[30] P. Liu, S. K. Au, Bayesian parameter identification of hysteretic behavior of composite walls, Probabilistic Engineering Mechanics 34 (2013) 101–109.

[31] D. D. Fitzenz, A. Jalobeanu, S. H. Hickman, Integrating laboratory creep compaction data with numerical fault models: A Bayesian framework, Journal of Geophysical Research: Solid Earth 112 (B8), B08410.

[32] W. P. Hernandez, F. C. L. Borges, D. A. Castello, N. Roitman, C. Magluta, Bayesian inference applied on model calibration of fractional derivative viscoelastic model, in: V. Steffen Jr, D. A. Rade, W. M. Bessa (Eds.), DINAME 2015-Proceedings of the XVII International symposium on dynamic problems of mechanics, Natal, 2015.

[33] H. Rappel, L. A. A. Beex, S. P. A. Bordas, Bayesian inference to identify parameters in viscoelasticity, Mechanics of Time-Dependent Materials 22 (2) (2018) 221–258.

[34] H. Rappel, L. A. A. Beex, Estimating fibres' material parameter distributions from limited data with the help of Bayesian inference, European Journal of Mechanics - A/Solids 75 (2019) 169 – 196.

[35] M. Mohamedou, K. Zulueta, C. N. Chung, H. Rappel, L. A. A. Beex, L. Adam, A. Arriaga, Z. Major, L. Wu, L. Noels, Bayesian identification of mean-field homogenization model parameters and uncertain matrix behavior in non-aligned short fiber composites, Composite Structures 220 (2019) 64–80.

[36] P. S. Koutsourelakis, A multi-resolution, non-parametric, Bayesian framework for identification of spatially-varying model parameters, Journal of Computational Physics 228 (17) (2009) 6184–6211.

[37] P. S. Koutsourelakis, A novel Bayesian strategy for the identification of spatially varying material properties and model validation: An application to static elastography, International Journal for Numerical Methods in Engineering 91 (3) (2012) 249–268.

[38] F. Uribe, I. Papaiannou, W. Betz, J. Latz, D. Straub, Bayesian model inference of random fields represented with the Karhunen-Loève expansion, in: UNCECOMP 2017 2 nd ECCOMAS Thematic Conference on Uncertainty Quantification in Computational Sciences and Engineering, 2017.

[39] A. Vigliotti, G. Csányi, V. S. Deshpande, Bayesian inference of the spatial distributions of material properties, Journal of the Mechanics and Physics of Solids 118 (2018) 74–97.

[40] S. Brooks, A. Gelman, G. Jones, L. X. Meng, Handbook of Markov chain Monte Carlo, CRC press, 2011.

[41] J. L. Beck, Bayesian system identification based on probability logic, Structural Control and Health Monitoring 17 (7) (2010) 825–847.

[42] C. E. Rasmussen, Gaussian processes in machine learning, Springer Science & Business Media, Berlin, Heidelberg, 2004, pp. 63–71.

[43] M. Sklar, Fonctions de répartition à n dimensions et leurs marges, Université Paris 8, 1959.

[44] R. d. S. Silva, H. F. Lopes, Copula, marginal distributions and model selection: A Bayesian note, Statistics and Computing 18 (3) (2008) 313–320.

[45] Y. Noh, K. K. Choi, I. Lee, Identification of marginal and joint CDFs using Bayesian method for RBDO, Structural and Multidisciplinary Optimization 40 (1) (2009) 35.

[46] H. Haario, E. Saksman, J. Tamminen, Adaptive proposal distribution for random walk Metropolis algorithm, Computational Statistics 14 (3) (1999) 375–396.